ORIGINAL ARTICLE

CrossMark

Three Cdk1 sites in the kinesin-5 Cin8 catalytic domain coordinate motor localization and activity during anaphase

Alina Goldstein[1] · Nurit Siegler[1] · Darya Goldman[1] · Haim Judah[1] ·
Ervin Valk[2] · Mardo Kõivomägi[2] · Mart Loog[2] · Larisa Gheber[1]

Abstract The bipolar kinesin-5 motors perform essential functions in mitotic spindle dynamics. We previously demonstrated that phosphorylation of at least one of the Cdk1 sites in the catalytic domain of the *Saccharomyces cerevisiae* kinesin-5 Cin8 (S277, T285, S493) regulates its localization to the anaphase spindle. The contribution of these three sites to phospho-regulation of Cin8, as well as the timing of such contributions, remains unknown. Here, we examined the function and spindle localization of phospho-deficient (serine/threonine to alanine) and phospho-mimic (serine/threonine to aspartic acid) Cin8 mutants. In vitro, the three Cdk1 sites undergo phosphorylation by Clb2-Cdk1. In cells, phosphorylation of Cin8 affects two aspects of its localization to the anaphase spindle, translocation from the spindle-pole bodies (SPBs) region to spindle microtubules (MTs) and the midzone, and detachment from the mitotic spindle. We found that phosphorylation of S277 is essential for the translocation of Cin8 from SPBs to spindle MTs and the subsequent detachment from the spindle. Phosphorylation of T285 mainly affects the detachment of Cin8 from spindle MTs during anaphase, while phosphorylation at S493 affects both the translocation of Cin8 from SPBs to the spindle and detachment from the spindle. Only S493 phosphorylation

affected the anaphase spindle elongation rate. We conclude that each phosphorylation site plays a unique role in regulating Cin8 functions and postulate a model in which the timing and extent of phosphorylation of the three sites orchestrates the anaphase function of Cin8.

Introduction

Chromosome segregation during mitosis is mediated by the dynamics of the mitotic spindle, a microtubule (MT)-based bipolar structure. Two types of MTs exist within the mitotic spindle, namely kinetochore MTs, which are captured at their dynamic plus-ends by kinetochores and control chromosome movement within the spindle [1], and interpolar MTs, which span the two spindle pole bodies (SPBs) and overlap in the middle region of the spindle, the midzone. Kinesin-5 motor proteins perform essential roles in mitotic spindle dynamics, such as assembly of the mitotic spindle, maintenance of the spindle structure and spindle elongation during anaphase B [2–6]. Kinesin-5 motors are unique, in that they function as homo-tetramers, with two catalytic motor domains being found on each pole of a double-coiled coil rod [7–10]. This unique structure enables kinesin-5 motors to perform their essential mitotic functions, specifically to crosslink and slide anti-parallel microtubules apart at the spindle midzone [11, 12]. *Saccharomyces cerevisiae* express two kinesin-5 homologs, Cin8 and Kip1, which perform partially overlapping functions, with at least one required for spindle assembly [13, 14]. However, Cin8 but not Kip1 was found to be essential for spindle assembly

✉ Larisa Gheber
lgheber@bgu.ac.il

1 Department of Chemistry and Ilse Katz Institute for Nanoscale Science and Technology, Ben-Gurion University of the Negev, PO Box 653, 84105 Beer-Sheva, Israel

2 Institute of Technology, University of Tartu, Tartu, Estonia

at elevated temperatures [2, 15]. In addition, Cin8 was shown to be crucial for anaphase progression [15–18], destabilization of interpolar MT plus ends [19] and kinetochore clustering [20–22].

Numerous studies have indicated that kinesin-related motor proteins are regulated by phosphorylation by several protein kinases, including glycogen synthase kinase-3β (GSK3β), Jun N-terminal kinase (JNK), cyclin-dependent kinase 1 (Cdk1) and Aurora A/B, polo kinase 1 (reviewed in [23–27]). However, the position, effect and mechanism of such phospho-regulation varies among the different kinesin-related motors [28–33]. One of the best-characterized kinesin motors is the axonal transporter kinesin-1, which mediates the transport of vesicles and organelles in neurons. Phosphorylation in the kinesin-1 light chain inhibits, either directly or indirectly, the ability of kinesin-1 to bind its cargo [34–36]. In addition, kinesin-1 is phosphorylated in its motor domain by p38 kinase and JNK, resulting in its reduced attachment to MTs [37–41]. Another well-studied kinesin is the MT-destabilizer kinesin-13, better known as mitotic centromere-associated kinesin (MCAK). Phosphorylation of MCAK by several major kinases has been reported in a range of organisms, revealing a complex network of regulation. MCAK is phosphorylated by Aurora B at several sites in its catalytic motor domain, affecting its localization and function [42–48]. Also, a specific site in the motor domain of *Drosophila* MCAK (S573) was found to be phosphorylated by casein kinase 1 alpha, which regulated the timing of MCAK activity in meiosis and mitosis [47]. Finally, phospho-regulation of the motor domain of *Xenopus laevis* MCAK by Cdk1 was found to promote release from centrosomes, thus regulating spindle formation [49].

Kinesin-5 motors have been also shown to undergo phospho-regulation in a number of organisms. The *X. laevis* kinesin-5 Eg5 was found to be associated with and phosphorylated by the Aurora-related protein kinase pEg2 [50]. Phosphorylation of a conserved BimC box motif at the C-terminus of kinesin-5 motors from *X. laevis*, *Drosophila melanogaster* and human by Cdk1 was found to positively regulate their interactions with MTs [5, 51–53]. In *Caenorhabditis elegans*, the kinesin-5 BMK-1 lacks the BimC box motif, however, phosphorylation at an analogous site by Aurora B kinase was found to recruit BMK-1 to mitotic and meiotic spindles [54]. Nevertheless, several kinesin-5 homologs, such as Cut7 and Cin8, were found to be exceptions, having no direct effect on interactions with MTs as a result of phosphorylation in the C-terminal domain of these kinases [55, 56]. Although it was initially established that kinesin-5 motors are phopho-regulated at their C-terminal tail domain [4, 50, 53, 57–59], Cin8 and KLP61F were found to be phospho-regulated at their catalytic motor domain. The *Drosophila* kinesin-5 KLP61F

was found to be phospho-regulated by Wee1 at three tyrosines found in the motor domain, with such regulation being essential [60]. On the other hand, *S. cerevisiae* Cin8 contains five putative Cdk1 phosphorylation sites, three of which are located in the N-terminal catalytic motor domain and two in the stalk and tail region [61]. We previously demonstrated that Cin8 is mainly regulated by phosphorylation of the three sites located in the motor domain [56]. We reported that phosphorylation at these sites affected the Cin8 localization to the mitotic spindle during anaphase B. Furthermore, we showed that a phospho-mimic mutant of Cin8 exhibited reduced binding to spindle MTs and impaired viability [56, 62]. This notion was recently supported by Roccuzzo et al., who demonstrated that in the absence of the activity of the Cdc14 phosphatase that dephosphorylates modified Cdk1 sites, Cin8 must carry phospho-deficient mutations of the Cdk1 sites in its catalytic domain for proper spindle elongation. Interestingly it was found that phosphorylation of the midzone organizing protein Ase1 [63] by Cdk1 inhibited the interaction of Cin8 with interpolar MTs [64], revealing the complex regulation of Cin8 spindle localization.

Two of the three Cdk1 phosphorylation sites in the motor domain which are implicated in regulation of Cin8 (i.e., S277 and T285) are located in a large 99 amino acid-long insert in loop eight that is unique to Cin8 [65, 66]. At the same time, the third site (S493) is conserved among most kinesin-5 motors [62]. Despite the well-established collective role of these three sites in Cin8 phospho-regulation, the contribution and influence of each individual site remains unknown. In the current work, we sought to dissect the mechanism of phospho-regulation at these sites by quantitatively examining the phenotypes of cells expressing Cin8 variants that carry single phospho-deficient mutations at each site. We show that phosphorylation of Cin8 affects two separate aspects of Cin8 localization to the spindle during anaphase, namely the release of Cin8 from the near-SPB region and its subsequent translocation to the interpolar spindle MTs, as well as release of Cin8 from interpolar MTs and the midzone. We further show that phosphorylation at the three Cdk1 sites in the Cin8 motor domain differentially affects these two aspects of phospho-regulation. Phosphorylation at S277 and S493 caused translocation of Cin8 from the near-SPB region to spindle MTs, while phosphorylation at T285 and S493 caused the release of Cin8 from spindle MTs. Phosphorylation at S277 is likely to occur first, as the phospho-deficient mutation at this site abolished translocation of Cin8 from the SPB region to the spindle MTs, along with the resulting release of Cin8 from the spindle. Based on these results, we propose a model for the function and timing of phosphorylation of each of the Cdk1 sites in the catalytic domain of Cin8.

Results

To study the roles of the different Cdk1 sites in the catalytic domain of Cin8 in regulating Cin8 function, we first performed phosphorylation assays to evaluate whether Cdk1 can phosphorylate the individual sites in vitro. For this purpose, in vitro phosphorylation of bacterially expressed motor domains of Cin8 variants by Clb2-Cdk1 was performed as previously described [56]. Five Cin8 variants were examined in which serine (S) or threonine (T) residues in the Cdk1 sites were changed to alanine (A). The following versions of Cin8 were tested: wt Cin8; Cin8-S277A T285A S493A (Cin8-3A); Cin8-T285A S493A; Cin8-S277A S493A; and Cin8-S277A T285A. In each double phospho-deficient mutant, only one of the three motor-domain phosphorylation sites was left active and could undergo phosphorylation. As can be seen (Fig. 1),
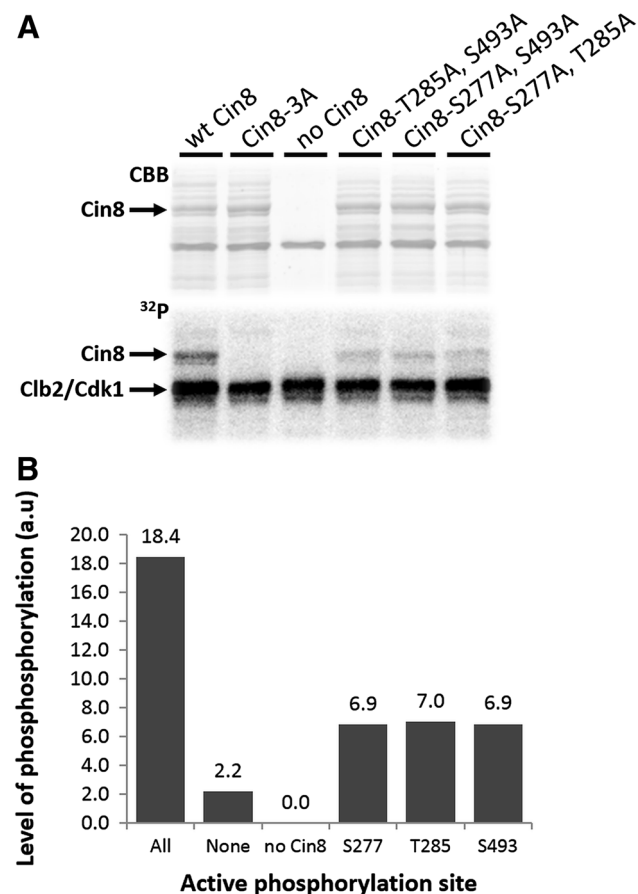

Fig. 1 In vitro Clb2-Cdk1 kinase assay of the Cin8 motor domain. **a** CBB staining and ^{32}P autoradiograms of SDS-PAGE fractionation of phosphorylation reaction mixtures with five phospho-variants of Cin8: wt; 3A; S277A, T285A; S277A, S493A; and T285A, S493A. The phosphorylation reaction mixture without Cin8 served as negative control. **b** Qualitative level of phosphorylation. The columns quantify phosphorylation band intensity, as measured on the autoradiogram. The columns are named after the active phosphorylation sites in each mutant; "None" refers to Cin8-3A, "All" to wt Cin8

the Cin8-3A mutant, in which all of the Cdk1 sites were removed, exhibited the lowest level of phosphorylation, likely due to non-specific phosphorylation at non-Cdk1 sites. The intensity of the phosphorylation band of wt Cin8 was the highest. The intensities of the phosphorylation bands of the double phospho-deficient mutants were intermediate, indicating that each of the three sites is accessible to Clb2-Cdk1.

Based on these results, we next sought to define the contributions of the different Cdk1 sites in the catalytic domain of Cin8 to its regulation. We compared the spindle localization of Cin8 phospho-deficient variants tagged with three tandem copies of green fluorescent protein (Cin8-3GFP) in which the target serine or threonine in one of the three Cdk1 sites in the motor domain was mutated to alanine (Fig. 2; Fig. S1). Consistent with our previous report [56], we found that wt Cin8 localized near the SPBs and spindle MTs in early mid anaphase, later detaching from the spindle, resulting in diffuse localization of the protein in the divided nuclei. Since Cin8 was reported to be a bi-directional motor [67, 68], its minus-end-directed motility likely led to clustering of Cin8 at the minus-ends of the MTs near the SPBs [69] while its plus-end-directed motility may be responsible for its enrichment at kinetochores [22] and/or short kinetochore MTs [20]. We refer to this localization as "near-SPB". In contrast to wt Cin8, the phospho-deficient Cin8-3A variant concentrated near the SPBs and at the midzone and did not detach from the spindles (Fig. 2i, ii; Fig. S1 i, ii), indicating that phosphorylation of at least one site in the Cin8 catalytic domain is required for its detachment from the near-SPB region and spindle MTs [56]. Analysis of the spindle localization of the different variants revealed significant asymmetry between Cin8 localization near the two SPBs (Fig. S2), with the bud-SPB having a more concentrated and higher intensity fluorescence signal, as compared to the mother SPB (Fig. S2, arrows). The less bright and concentrated fluorescence signal at the mother SPB was often correlated with more diffusive localization of Cin8-3GFP in the mother cell nucleus (Fig. 2i; Fig. S1 i, white arrow). It has been previously reported that during anaphase, Cdk1 is distributed asymmetrically between the two nuclei, and is present at higher concentrations in the mother cell [70]. Therefore, our data suggests that at least some of the asymmetry seen in Cin8 localization near the SPBs could be caused by Cin8 phosphorylation.

Comparing the spindle localization of single phospho-deficient mutants revealed that the Cin8-S277A mutant, like Cin8-3A, remained concentrated near the SPBs in short, intermediate and long anaphase spindles and became only slightly diffuse around one of the SPBs (Fig. 2iii; Fig. S1 iii, white arrow). On the other hand, anaphase spindle localization of the Cin8-T285A and Cin8-S493A
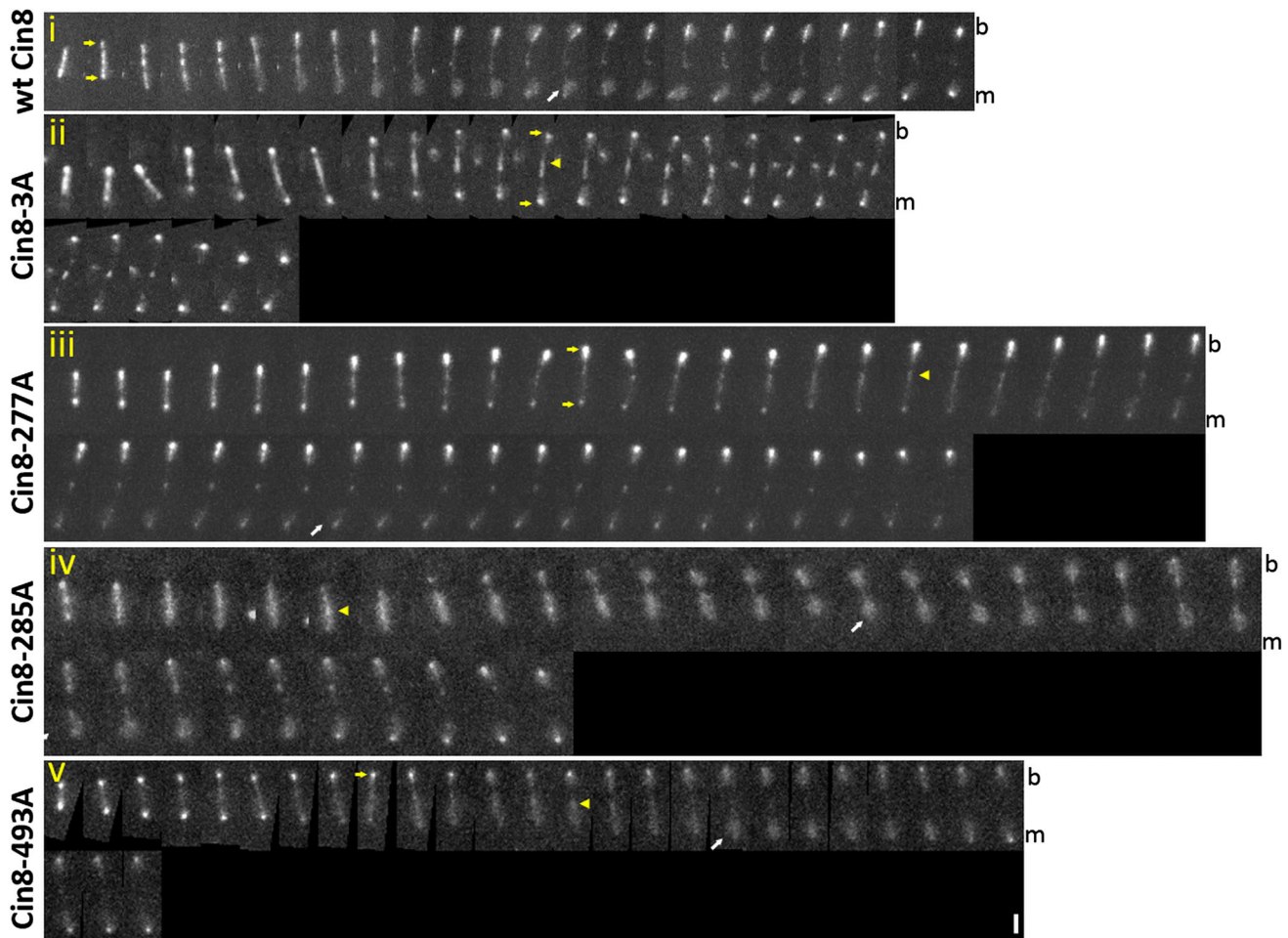
Fig. 2 Localization of Cin8 phospho-variants to anaphase spindles. Time-lapse 2D-projected images of anaphase spindle in Cin8-3GFP (wt and phospho-mutants)-expressing cell. Time intervals between frames—60 s. Cin8 and its mutants, indicated on the *left*, were integrated into a *LEU* locus in *cin8Δ* cells (Table S1). All cells are presented with the mother cell at the *bottom*. *Arrowheads* indicate the midzone of mitotic spindle; *yellow arrows* indicate Cin8 concentrated at the SPB, *white arrows* indicate diffuse Cin8 at the nucleus; *m* mother cell, *b* bud cell. *Scale bar* 2 μm

mutants roughly resembled the pattern of wt Cin8 localization (Fig. 2iv, v). However, the attachment of Cin8-S493A to the spindle MTs seemed to have increased in intermediate spindles, as compared to wt Cin8 (Fig. S1, v, arrowheads).

To quantitatively analyze the distribution of Cin8 variants along the anaphase spindles, we performed line-scan-analysis along spindles of various lengths in cells expressing 3GFP-tagged variants of Cin8 (Figs. 3b, 4, 5b; Fig. S3B, S4 and S6D). In all spindles, the fluorescent signal was interpolated and divided into one hundred segments of equal length which allowed us to calculate the average fluorescent signal along the spindle (see "Materials and methods" and [71]). In a line-scan plot, Cin8 fluorescence intensity peaked at about 10 and 90% of the spindle length, reflecting Cin8 localization at the SPBs (Figs. 3b, 4, 5b; Fig. S4, arrows). The smaller peak at about 50% of the anaphase spindle length represents Cin8 localization at the midzone (Figs. 3b, 4, 5b;

Fig. S4, arrowhead). Consistent with previous reports, the majority of Cin8 localized near the SPBs in pre-anaphase spindles, resulting in about fourfold higher average Cin8 fluorescence near the poles than at the middle of the spindle (Fig. 3; Fig. S3). With the onset of anaphase, at spindle lengths between 3 and 4 μm, Cin8 binding to spindle MTs increased (Fig. 4a; Fig. S4A), resulting in an increase in the Cin8 fluorescent signal at the middle of the spindle, relative to the mother SPB (Fig. 4a; Fig. S4A) and consistent with the notion that Cin8 relocates from the near-SPB region to the interpolar spindle MTs. In long spindles, Cin8 mainly concentrated near the SPBs and in the middle region of the spindle, the midzone (Fig. 4; Fig. S4). A similar pattern of Cin8 localization was seen in cells expressing wt Cin8-3GFP alone or in combination with tagged spindle-pole body-binding protein Spc42-tdTomato (Fig. 3). However, the binding of Cin8 to the midzone was considerably more pronounced in cells expressing Cin8-3GFP with Spc42-
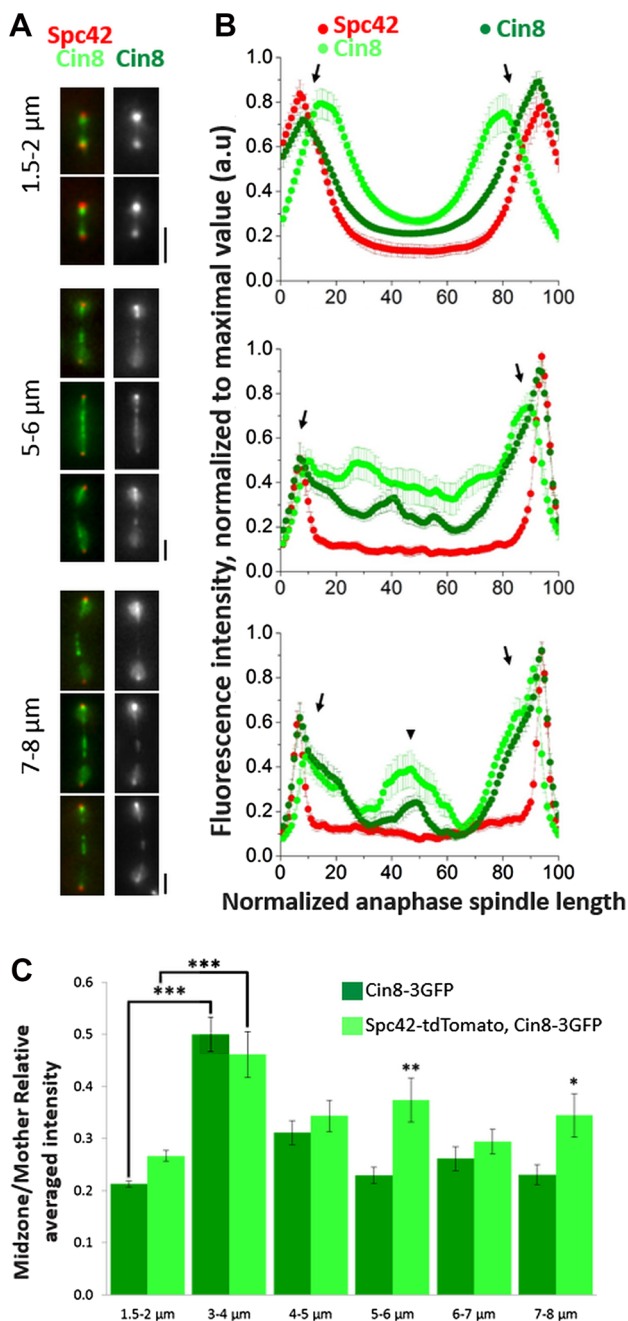
◀ **Fig. 3** Quantitative analysis of spindle Cin8 distribution on anaphase spindles during spindle elongation. **a** Representative images of spindles in cells expressing Cin8-3GFP alone or Cin8-3GFP with Spc42-tdTomato, at the different lengths indicated on the *left*. Tagged proteins are indicated on the *top*. *Scale bar* 2 μm. **b** Line-scan analysis along the spindle of cells expressing Cin8-3GFP with Spc42-tdTomato (*light green* and *red*, respectively) or Cin8-3GFP alone (*dark green*) at different spindle lengths, as per the representative images on the *left*. The fluorescence intensity along the spindle (*x*-axis) is measured from the mother to the bud cell and interpolated to 100 points of equal length. Spindle borders were determined either by the Spc42 fluorescence signal in cell expressing Spc42-tdTomato or by the bright Cin8 signal near the SPB, in cells expressing Cin8 alone. *Arrows* point to Cin8-3GFP intensity peaks at about 10 and 90% of the spindle length, while the *arrowhead* points to the Cin8-3GFP intensity peak at about 50% of spindle length. **c** Relative averaged intensity of Cin8-3GFP at the midzone (see "Materials and methods") in cells expressing Cin8-3GFP in the different spindle lengths categories with Spc42-tdTomato (*light green*) or Cin8-3GFP alone (*dark green*). Averages ± SEM of 10–20 spindles are shown at different spindle lengths as indicated at the *bottom*. *$P < 0.05$, **$P < 0.005$ and ***$P < 0.0005$

proteins tagged with fluorescent proteins, for reliable quantitative comparison of the phenotypes of the phospho-variants of Cin8, we used cells expressing these variants as the sole tagged protein.

Quantitative analysis of the distribution of the phospho-variants along the spindles revealed that while in pre-anaphase spindles of <2 μm the distribution of the phospho-variants of Cin8 was similar (Fig. S3), in the anaphase spindles, significant differences in the localization of the variants were observed (Fig. 4; Fig. S4). The Cin8-3A variant mainly concentrated at the SPBs (Fig. 4; Fig. S4, arrows) and the midzone (Fig. 4; Fig. S4, arrowheads), whereas wt Cin8 was also found on spindle MTs of all lengths but mainly in the short and intermediate anaphase spindles. This result indicates that phosphorylation of Cdk1 sites caused translocation of Cin8 from near-SPBs to the spindle MTs. The concentrated localization of the Cin8-3A mutant at the middle region is consistent with the high affinity of this mutant for MTs [56, 62]. It is likely that the increased concentration of the Cin8-3A mutant at the midzone resulted from Cin8 population that was bound to the overlapping MT region prior to the onset of anaphase, or from nascent Cin8-3A that bound to the midzone region, either directly or via Ase1 [64].

In early anaphase spindles 3–4 μm-long, binding of the Cin8-S277A and Cin8-S493A mutants to the spindle MTs was significantly lower, as compared to wt Cin8 binding, indicating that in these mutants, translocation of Cin8 from the near-SPB region to the spindle MTs was impaired (Fig. 4a). Interestingly, the midzone localization of the Cin8-S277A mutant was also lower than that of the Cin8-3A variant (Fig. 4a; Fig. S4A), suggesting that residual phosphorylation of the intact active sites, i.e. the T285 and/or S493 sites, was responsible for the detachment of Cin8

tdTomato than in cells expressing Cin8-3GFP alone (Fig. 3b, c), indicating that Cin8 detachment from the anaphase spindle MTs was diminished in cells expressing Cin8-3GFP with Spc42-tdTomato. This difference was most pronounced in the long anaphase spindles (Fig. 3b bottom, panels, c), indicating that in cells expressing Cin8-3GFP and Spc42-tdTomato, Cin8 concentrated at the midzone at the end of anaphase, which clearly contradicts previous reports stating that at the end of anaphase, Cin8 detaches from the midzone [56, 64, 71]. Since this discrepancy may result from a genetic alteration in cells containing two mitotic/cell cycle
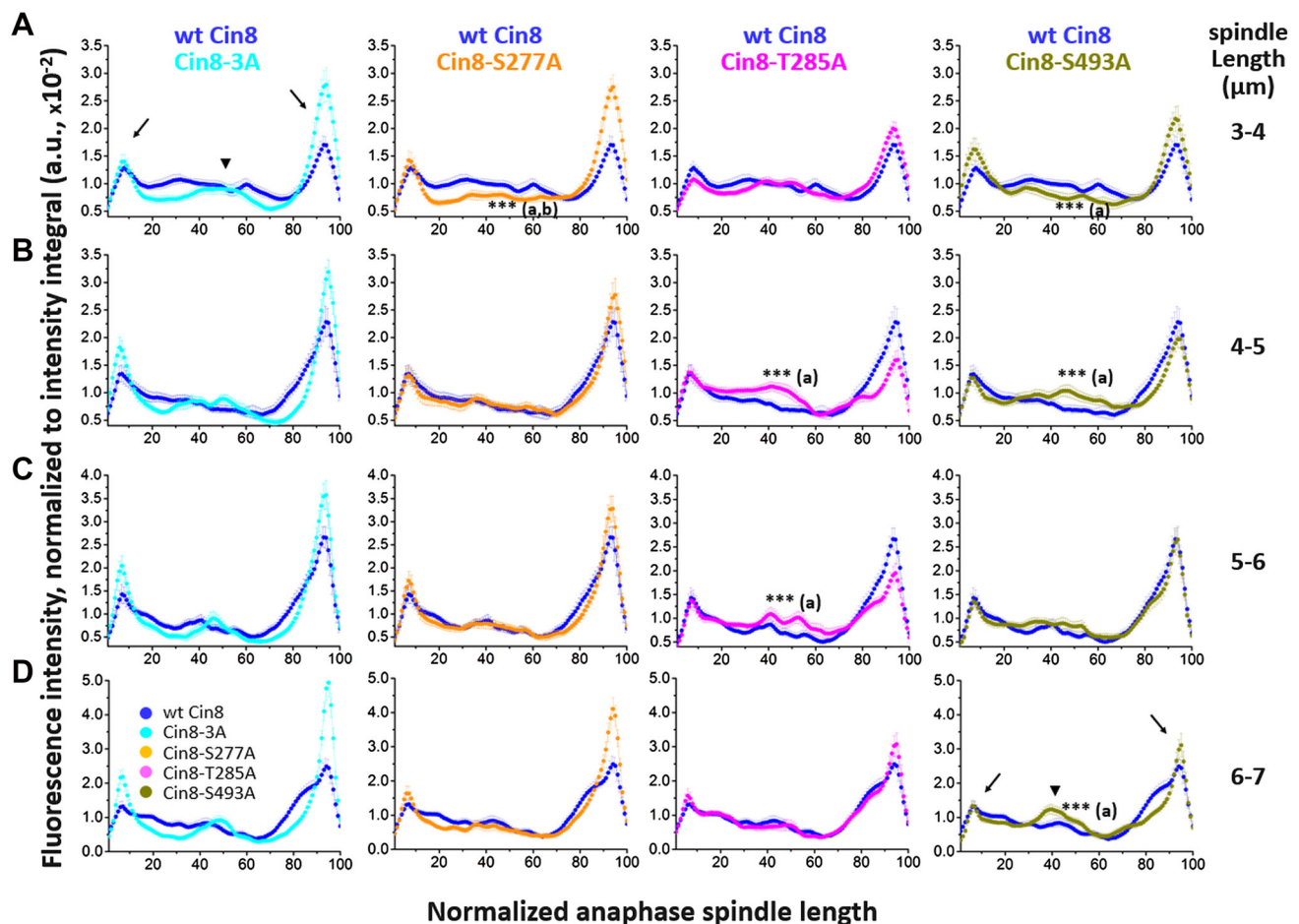
Fig. 4 Average fluorescence intensity along the spindle length of the three phospho-mutants, as compared to the fluorescence of wt Cin8. Spindle lengths categories are indicated on the *right*. Cin8-3GFP fluorescence intensity parallel to the spindle was measured starting at the mother cell, and divided to 100 points of equal length. The fluorescence of the background was subtracted from the Cin8-3GFP fluorescent signal, followed by normalization to the total integral of the Cin8-3GFP fluorescence signal. The signal for each mutant is compared to that of wt Cin8, indicated on *top*. *Black arrows* indicate intensity peaks at the SPBs while *arrowheads* point to intensity peaks at the midzone. The spindle length ranges are: **a** 3.0–3.9 μm; **b** 4.0–4.9 μm; **c** 5.0–5.9 μm; **d** 6.0–6.9 μm. For each length-segment, the average fluorescence intensity (±SEM) was determined for 14–20 cells. (*a*) Significance compared to wt Cin8. (*b*) Significance compared to Cin8-3A. ***$P < 0.0005$

from the midzone region. On the other hand, the spindle distribution of the Cin8-T285A mutant was similar to that of wt Cin8 (Fig. 4a; Fig. S4A), indicating that phosphorylation of the T285 site does not control the release of Cin8 from the SPBs in early anaphase. The localization of the S277A mutant along the spindle remained similar to that of the Cin8-3A mutant for all spindle lengths longer than 4 μm examined (Fig. 4b–d; Fig. S4B–D), indicating that phosphorylation at this site is critical for release of Cin8 from the near-SPB location. In intermediate spindles 4–6 μm in length, spindle MT-binding of the T285A mutant increased and became significantly higher than that of wt Cin8 (Fig. 4b, c; Fig. S4B, C). Such increased attachment to the spindle was likely caused by release from the SPBs upon phosphorylation of S277 and S493, where phosphorylation may be higher than in wt Cin8 in the

absence of an active T285 site, and by the higher affinity of the Cin8-T285A mutant to the spindle MTs. At intermediate anaphase spindle lengths of 4–5 μm, the spindle localization of the S493A mutant also increased, as compared to what was seen with short anaphase spindles (Fig. 4b; Fig. S4B). This pattern was likely caused by phosphorylation of S277, which caused the release of Cin8 from the near-SPB region and by the higher affinity of the Cin8-S493A mutant for the spindle MTs.

Our results indicate that phosphorylation at S277 and S493 caused release of Cin8 from the near-SPB region and that phosphorylation of T285 and S493 sites caused release of Cin8 from the spindle MTs (Fig. 4). To confirm these conclusions, we examined the spindle localization of Cin8 variant in which S277 and S493 were mutated to the negatively charged phospho-mimic aspartic acid (D) and
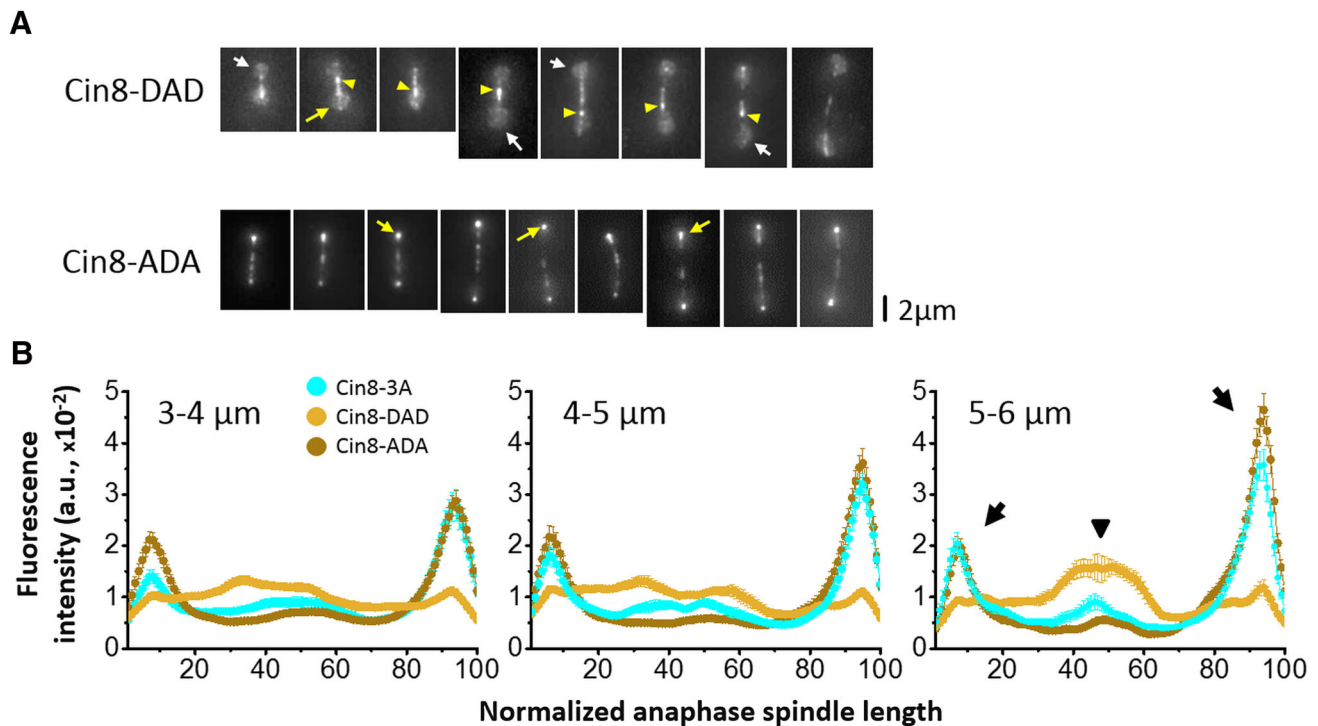
Fig. 5 Localization of Cin8 phospho-deficient/mimic variants to anaphase spindles. **a** Representative 2D projection of 3D stacks of fluorescent images of cells expressing 3GFP-tagged Cin8. Cin8-DAD (*top*) and Cin8-ADA (*bottom*). *Arrowheads* indicate Cin8 concentrating at the midzone of mitotic spindle; *yellow arrows* indicate Cin8 concentrated at SPB, while *white arrows* indicate diffuse Cin8 at the SPB. *Scale bar* 2 μm. **b** Cin8-3GFP fluorescence intensity parallel to the spindle, as in Fig. 4. The *x*-axis represents spindle length normalized to 100 length-segments and the *y*-axis represents Cin8-3GFP fluorescence intensity after the background was subtracted, followed by normalization to the total integral of the Cin8-3GFP fluorescence signal. For each length-segment, average fluorescence intensity (±SEM) was determined for 18–20 cells

T285 contained a phospho-deficient mutation to alanine (Cin8-DAD). Indeed, in anaphase spindles, this mutant exhibited extensive diffuse localization, with almost no binding to the near-SPB region, and remained bound to the midzone region (Fig. 5). Consistently, variant of Cin8 containing a phospho-mimic mutation at T285 and phospho-deficient mutations at S277 and S493 (i.e., Cin8-ADA) exhibited concentrated localization to the near-SPB region, as well as to interpolar and midzone MTs, yet showed almost no release from the spindle (Fig. 5).

Line-scan analysis along the spindle allowed us to compare the spindle attachment of the different mutants. To quantify differences in the detachment from anaphase spindles, we performed analysis of the Cin8 fluorescent signal along a line perpendicular to the spindle and close to the SPBs (Fig. 6). In this analysis, we did not take into account the signal at the middle of the fluorescence profile since this signal most likely resulted from the fluorescence of Cin8-3GFP attached to the near-SPB region and/or the spindle MTs (Fig. 6a). By this method, we only quantified the fluorescent signal of Cin8 that was diffusely localized to the nucleus following its detachment from the spindle (Fig. 6a). Such analysis was performed as a function of

time following the onset of anaphase, using time-lapse images of spindle elongation measurements in cells expressing 3GFP-tagged phospho-variants of Cin8 (Fig. S5A), which were also used to calculate the rate of anaphase spindle elongation (Table 1). We first compared the detachment of wt Cin8 and Cin8-3A in mother and bud cells (Fig. 6b). As expected, wt Cin8 fluorescence in the nucleus increased with time, peaking some 12 min following the onset of anaphase. The subsequent decrease in Cin8 fluorescence was likely due to degradation of the protein at later stages of anaphase [72]. We also found that Cin8 fluorescence in the nucleus of the mother cells was significantly higher than in the bud cells, consistent with increased Cdk1 phosphorylation of Cin8 in the mother cell (Figs. S1 and S2). The nuclear fluorescent signal of the phospho-deficient Cin8-3A mutant was significantly lower than that of wt Cin8, yet similar in the mother and bud cells (Fig. 6b). This result further supports the notion that the increased diffuse localization of Cin8 in the mother nucleus was dependent on Cdk1 phosphorylation.

Since our data indicated that the phosphorylation-dependent release of wt Cin8 was more pronounced in the mother than in the bud cell (Fig. 6b), we next compared
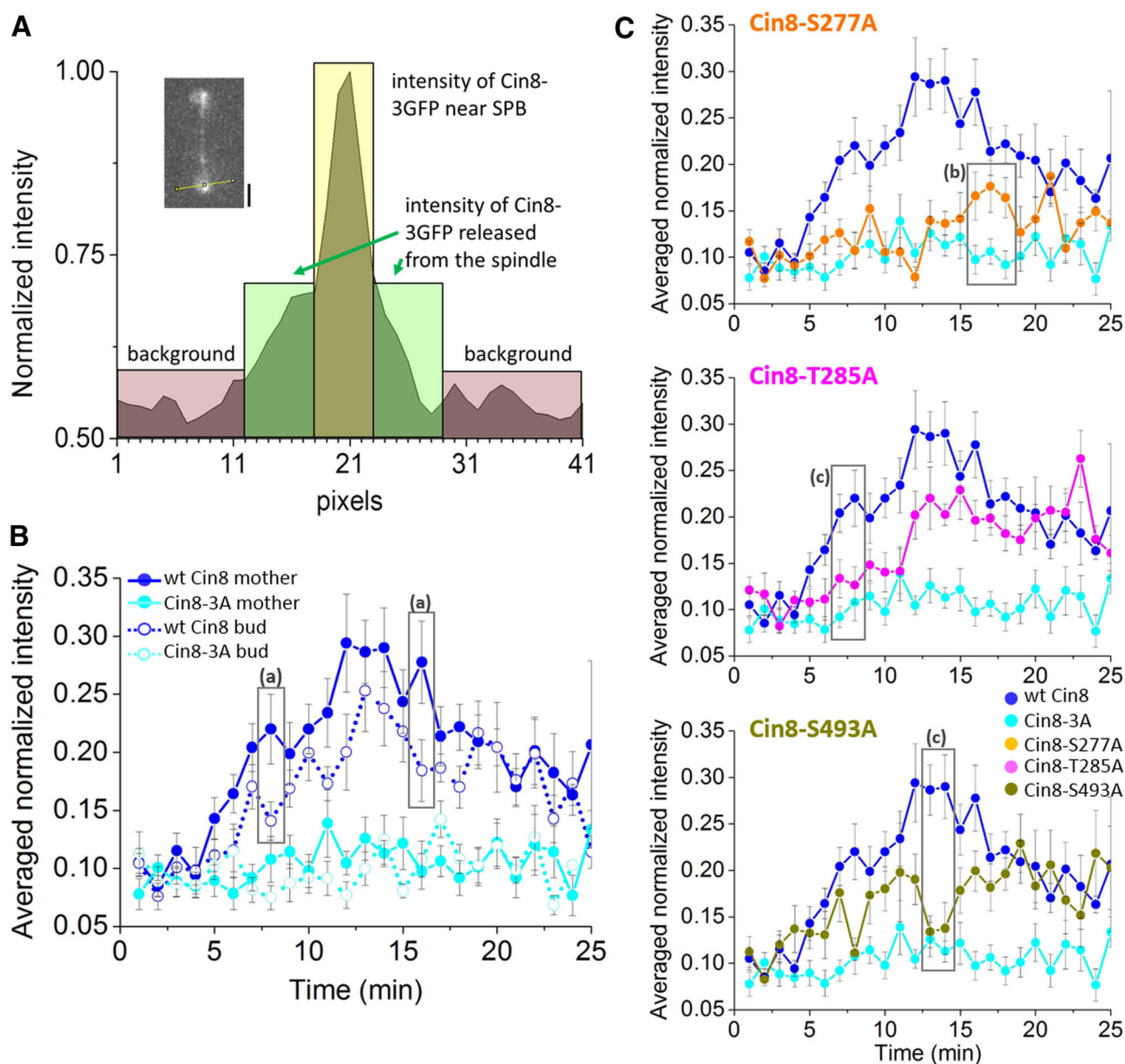
Fig. 6 Quantitative analysis of the detachment of Cin8 phospho-variants from mitotic spindles during anaphase. **a** Presentation of the method: line-scan measurements perpendicular to the spindle were performed on a single time point near the mother SPB. The corresponding image is shown at the *top left*; the *scale bar* represents 2 μm. The *y*-axis represents the intensity measured along the yellow line; the *x*-axis represents the pixels along this line. The intensity peak at 20 pixels corresponds to the high intensity of Cin8-3GFP near the SPB (*yellow rectangle*). Background intensity is indicated by *burgundy* was assigned as the background. The intensity indicated in *green* represents the intensity of Cin8-3GFP detached at the

nucleus; this intensity was averaged and normalized per time point for each cell (see "Materials and methods"). **b** The average intensity of Cin8 released from the spindle of wt Cin8 (*blue*) and Cin8-3A (*cyan*) in mother (*solid line*) and bud (*dashed line*) cells versus time (min) following the onset of spindle elongation. **c** Anaphase release of the three phospho-mutants from the spindle, as compared to wt Cin8 and Cin8-3A. **b**, **c** At each time point, the average intensity ± SEM of 9–12 cells is presented. *Gray* frames contain data points with $P < 0.05$, (*a*) significance compared between wt Cin8 fluorescence in the mother and bud cells; (*b*) significance compared to Cin8-3A or (*c*) wt Cin8

release of the single phospho-deficient mutants from the spindle in mother cells (Fig. 6c). We found that the Cin8-S277A mutant exhibited the lowest degree of release from the spindle, since its signal in the nucleus was lower than that of wt Cin8 throughout the duration of anaphase

(Fig. 6c, top). However, at later time points during anaphase, the release of this mutant from the spindle was significantly higher than that of the Cin8-3A mutant (Fig. 6c, top, gray frame), indicating that phosphorylation of T285 and/or S493 partially contributed to the release of

Table 1 Characteristics of anaphase spindle elongation in cells expressing Cin8 phospho-variants

Cin8 variant	Elongation rate (μm/min) (n)		Time before spindle disassembly (min) (n)
	First fast phase	Second slow phase	
wt Cin8	0.83 ± 0.04 (11)	0.25 ± 0.02 (10)	20 ± 1 (12)
Cin8-3A	0.81 ± 0.05 (11)	*0.35 ± 0.04 (9)	22.5 ± 0.7 (10)
Cin8-S277A	0.76 ± 0.07 (11)	0.30 ± 0.04 (11)	***29 ± 1 (10)
Cin8-T285A	0.74 ± 0.06 (10)	0.20 ± 0.03 (10)	***29 ± 2 (9)
Cin8-S493A	**0.65 ± 0.05 (10)	0.23 ± 0.02 (10)	**26 ± 1 (10)

Averages ± SEM of elongation rates during the fast and the slow phases and the time before spindle disassembly are presented. * $P < 0.05$, ** $P < 0.005$ and *** $P < 0.0005$, as compared to wt Cin8. In cells expressing the single mutants, the time before spindle disassembly is significantly longer than in cells expressing wt Cin8 or Cin8-3A

Cin8 from the spindle. Release of the Cin8-T285A mutant into the nuclei was delayed, relative to that of wt Cin8, but reached wt Cin8-like levels at later stages of anaphase (Fig. 6c, middle). This delay is consistent with the increased attachment of the Cin8-T285A mutant to the MTs in 4–6 μm-long intermediate anaphase spindles (Fig. 4b, c), supporting the notion that phosphorylation at this site regulates the attachment of Cin8 to MTs in early mid anaphase. Finally, the nuclear localization of the Cin8-S493A mutant was lower than that of wt Cin8 during middle anaphase (Fig. 6c, bottom), suggesting a partial influence of phosphorylation at this site on the detachment of Cin8 from anaphase spindle MTs.

Cin8 was found to play crucial roles in spindle assembly and anaphase spindle elongation [2, 11, 13, 15, 18]. Thus, we considered how the phosphorylation of different sites affected Cin8 function during critical stages of spindle dynamics (Fig. 7; Fig. S5; Table 1). Since Cin8 was found to be synthetically lethal with the overlapping kinesin-5 Kip1 and the midzone-organizing Ase1 [63], we first examined viability of cells carrying double chromosomal deletions of cin8Δkip1Δ and cin8Δase1Δ and covered by a plasmid expressing wt and phospho-variants of Cin8 (Fig. 7a). We found no difference in the viability of cells expressing the Cin8 phospho-variants in these cells (Fig. 7a top and bottom, respectively), indicating that the major overlapping functions of Cin8 and Kip1 and Cin8 and Ase1 are not affected by phosphorylation in the catalytic domain of Cin8. Since it was demonstrated that the viability of cells expressing Cin8 mutants as sole source of kinesin-5 function closely correlated with the ability of these mutants to assemble mitotic spindles [2, 14], we concluded that the lack of phosphorylation of individual Cdk1 sites in the catalytic domain of Cin8 did not interfere with the spindle assembly function of Cin8. Examination of spindle morphology distribution in budded cells (Fig. 7b) revealed that cells expressing the Cin8-S277A mutation accumulated with pre-anaphase spindles (Fig. 7c), indicating that the onset of anaphase was delayed in these cells.

We have also shown here that in short anaphase spindles, spindle attachment of the Cin8-S277A mutant was lower than that of the wt Cin8 and the Cin8-3A mutant (Fig. 4a; Fig. S4A). Thus, the delayed entry of cells expressing the Cin8-S277A mutation into anaphase (Fig. 7c) may be an outcome of insufficient SPB-separation caused by the reduced amount of the Cin8-S277A mutant on the spindle/midzone MTs, compared to the other phospho-variants of Cin8. Alternatively, expression of the Cin8-S277A mutant could transiently activate the spindle assembly checkpoint [73–75], delaying the onset of anaphase.

To examine the function of the single mutants during anaphase spindle elongation, we followed their localization by time-lapse analysis and measured spindle elongation rates based on the fluorescent signal of Cin8 at the spindles (Fig. S5). Spindle elongation of all variants followed typical bi-phasic kinetics [17, 18] (Fig. S5B), allowing us to determine the average spindle elongation rate from these time-lapse sequences (Table 1). Consistent with our previous report [56], we found that the spindle elongation rate in the second phase of anaphase B was faster in cells expressing the Cin8-3A mutant, as compared to cells expressing wt Cin8 (Table 1). None of the single mutants alone could recapitulate this effect, indicating that phosphorylation at all three sites has overlapping effects on the rate of spindle elongation, likely through regulation of the attachment of Cin8 to the midzone region. Interestingly, in cells expressing only the Cin8-S493A mutant, the spindle elongation rate during the first (fast) phase of anaphase B was significantly slower than in cells expressing wt Cin8 (Table 1). This effect could result from detachment of Cin8 from the spindle due to the phosphorylation of S277 and T285 or from the slower MT-sliding activity of the Cin8-S493A mutant.

The serine at position 277 also fits the TURK consensus sequence RxxS which was reported to be specific for phosphorylation by the Dbf2/Dbf20 kinase (Fig. S6A), whose activity is important in the mitotic exit network (MEN) pathway [76]. Moreover, it was reported that like

Fig. 7 Viability and spindle morphology in cells expressing Cin8 phospho-variants. **a** Growth of a shuffle *cin8Δkip1Δ* (*top*) and *cin8Δase1Δ* (*bottom*) strains on plates containing 7.5 µg/mL cyclohexamide, following transformation with CEN plasmids expressing the different Cin8 phospho-variants (indicated on the *left*). Cells were plated in serial dilution at 26 and 37 °C. **b** Representative images of fixed immunostained cells showing tubulin and DNA morphologies in the different spindle length categories: monopolar, pre-anaphase (<2 µm), intermediate anaphase (2–5 µm), and long anaphase (>5 µm) spindles. The *scale bar* represents 2 µm. **c** Distribution of spindle lengths in budded cell expressing phosphorylation mutants of Cin8. In each genotype, a total of 300 cells was counted. Budded cells were classified into four morphology classes according to spindle morphology and length, as in **b**. *Columns* and *bars* represent average ± SEM of three independent experiments. *$P < 0.05$

Cin8 S277, one of the Cdk1 sites of the spindle-positioning protein Kar9 also fits the consensus for recognition by the Dbf2/Dbf20 kinase, which is involved in the regulation of Kar9 MT localization [77]. Thus, we performed experiments to examine the effect of mutation in the Dbf2/20 consensus on the localization of Cin8 to anaphase spindles (Fig. S6). For this purpose, we examined the function and localization of the Cin8-R274A mutant in which a critical arginine residue in the Dbf2/Dbf20-consensus sequence

was mutated to alanine. A similar mutation was previously shown to abolish phosphorylation by Dbf2/Dbf20 [78]. We found that this mutation did not affect the viability of cells when expressed as a sole source of kinesin-5 function (Fig. S6B), exhibiting similar spindle localization during anaphase as did wt Cin8 (Fig. S6C) and translocated from the near-SPB region to spindle MTs in early anaphase (Fig. S6D, top panel). These results indicate that the lack of translocation of the Cin8-S277A mutant from the near-SPB

region to spindle MTs in early anaphase (Fig. 4a) and release from the spindle at late anaphase (Fig. 2a) did not result from a lack of phosphorylation by Dbf2/Dbf20. These results further support the notion that phosphorylation by Cdk1 at the S277 site governs the localization of Cin8 to the spindle during anaphase spindle elongation.

In summary, our analysis reveals that each one of the Cdk1-specific sites in the catalytic domain of Cin8 control its attachment to and detachment from anaphase spindles in a unique manner, with the S277 site exerting the strongest effect on Cin8 localization to anaphase spindles.

Discussion

In this study, we quantitatively characterized the effects of multiple Cin8 phosphorylation at the three Cdk1 sites located in the motor domain of the protein and demonstrated distinct functions for each site. We showed that phosphorylation of Cin8 affects two separate aspects of Cin8 localization to the spindle during anaphase. First, phosphorylation affects the release of Cin8 from the near-SPB region and its relocation to interpolar MTs. Prior to the onset of anaphase, when Cin8 is dephosphorylated [56], the majority of Cin8 accumulated near the SPBs, with only a small amount being located on interpolar MTs. However, following the onset of anaphase, localization of wt Cin8 at the SPBs decreased, while on interpolar MTs, Cin8 levels increased (Figs. 2, 3, 4; Figs. S1, and S3–S4). This shift was abolished with the phospho-deficient mutant Cin8-3A, indicating the importance of Cin8 phosphorylation for this relocation event (Fig. 4; Fig. S4). Second, and consistent with a previous report [56], we showed that phosphorylation of Cin8 caused its release from interpolar MTs and from the midzone (Figs. 2, 4; Fig. S4). We further showed that phosphorylation at the three Cdk1 sites in the motor domain of Cin8 differentially affected these two aspects of phospho-regulation.

In spite of the fact that the three Cdk1 sites, S277, T285 and S493, undergo similar phosphorylation in vitro (Fig. 1), their role in regulating Cin8 function during anaphase in cells is different. A phospho-deficient mutant at the S277 site, exhibited significantly reduced translocation from the near-SPBs region to spindle MTs throughout anaphase, similarly to the phospho-deficient mutant Cin8-3A (Figs. 2iii, 4; Figs. S1 iii and S4). Consequently, this mutant also exhibited reduced detachment from the near-SPBs region (Fig. 6c), indicating that phosphorylation at this site serves as a major regulator of Cin8 spindle localization during anaphase and is likely to undergo phosphorylation prior to such modification at the T285 and S493 sites. S493, which is conserved in most kinesin motors, also contributes to regulating Cin8 localization and

appears to undergo phosphorylation mainly during early to mid-anaphase. In 3–4 μm-long spindles in early anaphase, phosphorylation at S493 affected the release of Cin8 from the near-SPB region (Fig. 4a, right). At mid-anaphase, when spindles are 4–5 μm long, phosphorylation at this site contributed to Cin8 detachment from midzone MTs (Fig. 4b; Fig. S4B). In contrast to S277 and S493, phosphorylation at T285 site mainly affected the affinity of Cin8 to interpolar MTs in intermediate spindles 4–6 μm in length (Fig. 4b, c, 5; Fig. S4B, C). Thus, we demonstrated here that phosphorylation of S277 and S493 causes release of Cin8 from the SPBs, while phosphorylation of T285 and S493 releases Cin8 from the midzone (Figs. 4, 5; Fig. S4). It is possible that cooperation between the phosphorylation of the different sites (i.e. S277 and T285 and/or S277 and the S493) produces the overall effect of phospho-regulation of the localization to and detachment from the anaphase spindles.

The differential effects and timing of phosphorylation of the different sites likely result from the positions of the different sub-domains in which these sites are located. Based on sequence alignment, the S277 and T285 sites are located within loop eight, while the S493 site is located in loop fourteen of the catalytic domain of kinesin motor proteins [66]. It was previously demonstrated that upon integration with MTs, loop eight of kinesin motors faces the MT lattice, while loop fourteen is located away from the MT lattice, in the vicinity of the ATP-binding P-loop [79]. The large distance between these two regions may result in differential accessibility to Cdk1 prior to and during anaphase. Moreover, prior to metaphase-to-anaphase transition, Cin8 accumulates in clusters near the SPBs (Fig. S3). This clustering can be induced by specific interaction between Cin8 tetramers, as recently suggested by us [69], or between Cin8 and another, yet unidentified protein leading to the exposure of S277 to phosphorylation by Cdk1 to a greater extent, as compared to the other sites. Similarly, at the midzone, Cin8 interaction with the MTs or with other spindle-binding factors, such as the midzone-organizing Ase1 [64], can also be differentially affected by phosphorylation at the different sites, depending on their spatial accessibility. A mechanism of differential regulation by phosphorylation of different sites by a specific kinase was previously demonstrated for the kinesin-13 MCAK from *X. laevis*, phosphorylated by the mitotic Aurora B kinase at three sites that control its function and localization [44–46]. Phosphorylation of one of these sites in MCAK yields stronger phenotypes than elicited by the others. Moreover, each site is phosphorylated at different stages of the cell cycle and at different locations in the cell [80]. Similarly, we demonstrated that S277 plays a dominant role in Cin8 regulation. Of the two sites located in a large insert in Cin8 loop eight, S277 site is conserved

within fungi, which divide via "closed mitosis" and contain inserts in loop eight, like Cin8 [62]. Therefore, we suggest that the phospho-regulation of Cin8 S277 may have evolved to support fungal kinesin-5 motor activity in "closed mitosis".

Previous reports demonstrated that Cin8 is a bidirectional kinesin that can switch its directionality under various experimental conditions [67, 68, 81, 82]. Recently, we proposed a physiological role for this motility characteristic whereby, prior to spindle assembly, the minus-end-directed motility of Cin8 is required for accumulation of Cin8 in clusters near the SPBs. Such clustering promotes the capture and sliding apart of anti-parallel MTs emanating from the neighboring SPB, which is essential for bipolar spindle formation [69]. We have also previously demonstrated [56] that in cells with short pre-anaphase spindles, Cin8 is dephosphorylated by the PP2A^{Cdc55} phosphatase [83]. Based on the current results, we propose that dephosphorylation of Cin8 prior to anaphase by PP2A^{Cdc55} is important for Cin8 accumulation near the SPBs, for spindle assembly and attachment to interpolar MTs and for maintenance of the bipolar spindle structure [56]. Following the onset of anaphase, the sister chromatid-separating protease separase [84] down-regulates the PP2A^{Cdc55} phosphatase [83]. This decrease in PP2A^{Cdc55} activity may allow partial phosphorylation of Cin8 by Cdk1 at S277, followed by phosphorylation at S493, which subsequently causes Cin8 release from the near-SPB region (Fig. 8). It has also been demonstrated [56, 85] that Cin8 is a target for the Cdc14 phosphatase, which is released during early anaphase by the FEAR pathway [86, 87]. The phospho-deficient Cin8-3A mutant was shown to suppress the requirement for Cdc14 and the polo kinase Cdc5 during anaphase spindle elongation [85]. Since we have shown that dephosphorylation at T285 and S493 induced the attachment of Cin8 to spindle MTs (Fig. 4), we propose that Cdc14 phosphatase targets these sites in early mid anaphase to promote Cin8 attachment to the spindle MTs, thus allowing proper spindle elongation. We further propose that at the onset of anaphase, the balance between the phosphorylation/dephosphorylation activities of Cdk1/Cdc14 allows release of Cin8 from the near-SPB region and promotes its attachment to spindle MTs (Fig. 8). Furthermore, since transcription of Cin8 is likely to continue throughout anaphase, the Cdk1/Cdc14 activity balance is important for targeting newly transcribed Cin8 to the spindle in early anaphase. Finally, we have previously demonstrated that Cin8 is differentially phosphorylated in late anaphase and that such phosphorylation is abolished by the phospho-deficient mutation Cin8-3A [56]. It was also previously shown that at mid-late anaphase, when the nuclei are separated,

Cdc14 is depleted from the midzone region [88, 89]. Thus, at this stage, Cin8 can be phosphorylated by residual Cdk1 activity near the midzone or by another kinase at the midzone, causing its detachment from midzone MTs.

The MT-binding spindle midzone-organizing protein Ase1 [63, 90] was previously shown to affect the spindle localization of Cin8 [64]. In early anaphase, Cin8 localization to the midzone was shown to be induced by dephosphorylation of the Ase1 Cdk1 sites [64]. Based on the results presented here, we further propose that the local balance of Cdk1/Cdc14 activity during anaphase precisely regulates the phosphorylation states of Cin8 and Ase1 and hence, the interaction and function of these proteins. A similar mechanism has been demonstrated for kinesin-6 and Ase1 in fission yeast [91].

The relationship between the spindle localization of Cin8 and its contribution to SPB-separation during anaphase is not clear. On the one hand, it has been demonstrated that in cells lacking Cin8, the rate of the first fast phase of anaphase B was significantly reduced, relative to what is seen in parent strain cells [18]. The expression of a Cin8 mutant defective in its MT-binding ability [11] produced a similar effect [17]. These results indicate that binding of Cin8 to midzone MTs increases the rate of spindle elongation. On the other hand, it has been demonstrated that enrichment of Cin8 at the spindle midzone in chromosome passenger complex mutant cells slows down anaphase B spindle elongation, suggesting that Cin8 serves as a brake during anaphase B in these cells [92]. In higher eukaryotes, kinesin-5 motors have also been suggested to function as a brake, slowing down spindle elongation during anaphase B [93, 94]. Consistent with a previous report [56], we showed that in late anaphase cells, the phospho-deficient Cin8-3A mutant is specifically enriched in the midzone (Figs. 2i, ii, 4d; Fig. S1i, ii, yellow arrowheads) and the rate of anaphase is faster than in parent strain cells (Table 1). These results indicate that the binding of Cin8 at the midzone induces anti-parallel sliding and contributes to an increased elongation rate. However, in early mid anaphase (spindle length, 4–5 μm), the increased levels of attachment of the Cin8-T258A and Cin8-S493A mutants to the spindles (Fig. 4b) did not result in increased rates of spindle elongation (Table 1). Based on this observation, we speculate that a minimal amount of Cin8 binding is required to drive efficient elongation in anaphase B, yet beyond this level of binding, no further acceleration of elongation occurs. Interestingly, Cin8-S493A was the only variant that exhibited significantly reduced spindle elongation rates during the first phase of spindle elongation (Table 1), which implies that phosphorylation of S493 regulates the kinetic properties of Cin8.

Fig. 8 Model of Cin8 phospho-regulation during mitosis. Cin8, SPBs and MTs are illustrated. *Yellow* and *black circles* indicate phosphorylated and dephosphorylated sites (S277, T285, S493), respectively. Major phosphorylated species of Cin8 are indicated on the *left* of each panel. **a** In pre-anaphase spindles, Cin8 is dephosphorylated by PP2A^{Cdc55} [83], resulting in its accumulation at near-SPBs regions [69]. **b** In early anaphase, PP2A^{Cdc55} is inactivated by separase [83] and the local balance of Cdk1/Cdc14 near the SPBs favors Cdk1. Cin8 undergoes partial phosphorylation at the S277 site, causing Cin8 release from near-SPB sites and its relocation to spindle MTs. **c** During early mid anaphase, S277 and S493 undergo phosphorylation, causing additional relocation of Cin8 from the SPBs to the midzone. Release of the Cdc14 phosphatase by the FEAR pathway [87, 89] likely shifts the local Cdk1/Cdc14 balance at the midzone towards Cdc14, keeping Cin8 (and Ase1, not shown) mainly de-phosphorylated at the T285 and S493 sites. This promotes Cin8 attachment to midzone MTs allowing spindle elongation during the first, fast phase of anaphase B. **d** In late anaphase, Cin8 is detached from the midzone and SPBs as a result of phosphorylation at all three sites in the motor domain [56]
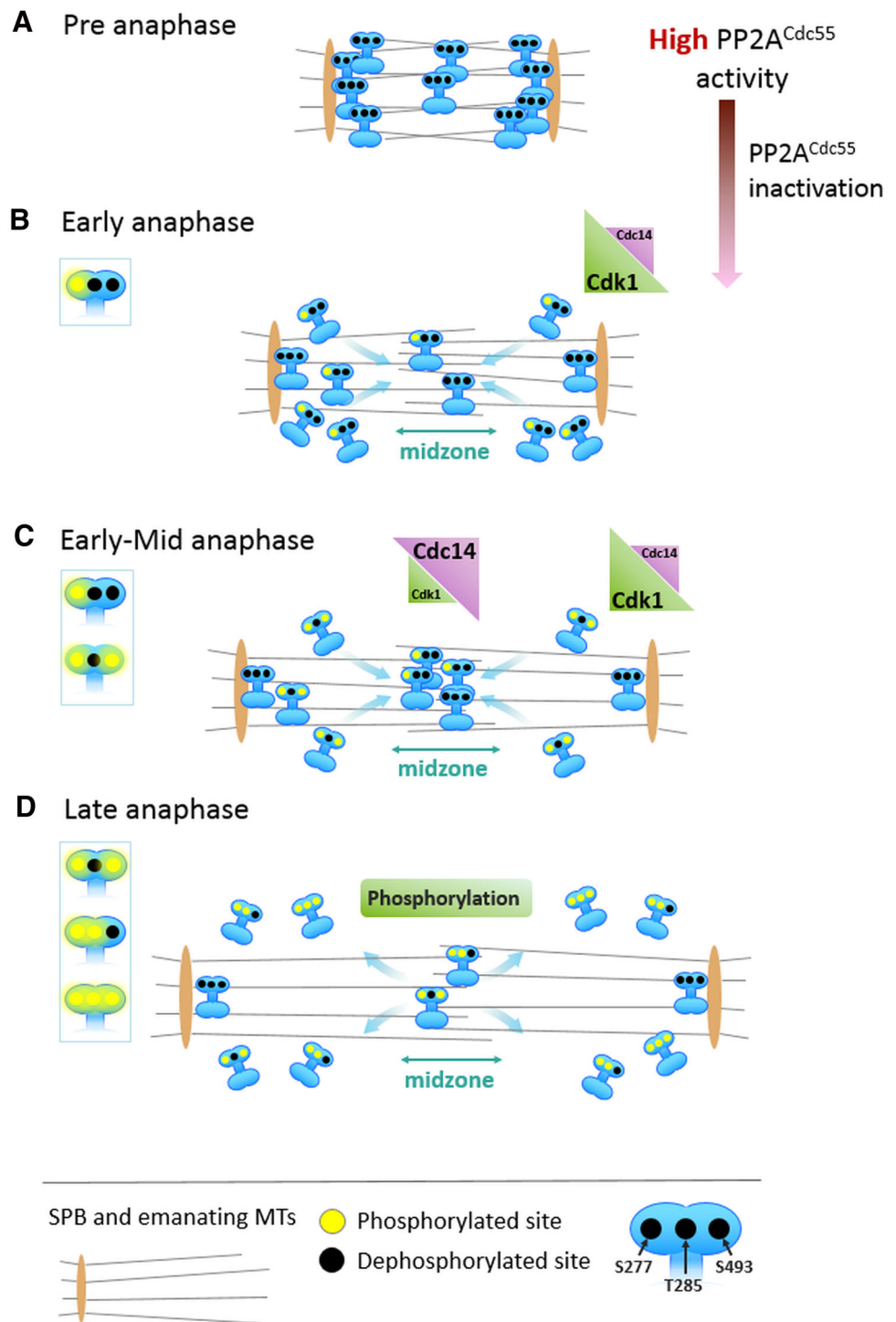
To summarize, we propose that phosphorylation of the three Cdk1 sites in the Cin8 motor domain regulates and coordinates both the localization of Cin8 at the anaphase midzone/spindle MTs and the activity of Cin8. This complex phospho-regulation, together with contributions from other factors [92], governs SPB separation and spindle elongation during anaphase.

Materials and methods

In vitro phosphorylation assay

In vitro phosphorylation assays were performed as previously described [56]. In brief, bacterially expressed Cin8 (590)-TEV-EGFP-6His variants were purified using

standard nickel affinity chromatography, with elution being accomplished with 300 mM imidazole that was subsequently removed using Zeba Spin Desalting Columns 40 K (Thermo Scientific). For a phosphorylation assay, equal concentrations of Cin8 variants were mixed with TAP-purified Clb2-Cdk1-Cks1 complex in kinase assay mixture [50 mM HEPES, pH 7.4, 150 mM NaCl, 5 mM MgCl$_2$, 8% glycerol, 0.2 mg/mL BSA, 500 nM Cks1 and 500 μM ATP (with added γ-^{32}P-ATP (PerkinElmer)]. Reactions were stopped after 10 and 20 min with SDS-PAGE sample buffer and proteins were separated by SDS-PAGE. Gels were stained with Coomassie Brilliant Blue (CBB) R-250 (Sigma) and incorporation of ^{32}P into the proteins was visualized by autoradiography.

Live cell imaging

The *S. cerevisiae* strains and plasmids used in this study are described in SI Tables S1 and S2. Live cell imaging was performed as previously described [16, 17, 56]. Cells were grown overnight in medium lacking uracil and tryptophan. Two hours prior to imaging, the cells were diluted tenfold. Images were acquired using a Zeiss Axiovert 200 M-based microscope setup equipped with a cooled CCD Andor Neo sCMOS camera. Images of Z stacks of eleven planes were obtained in three channels with 0.5 μm separation. Time-lapse images were obtained using a Zeiss Axiovert 200 M-based Nipkow spinning-disc confocal microscope (UltraView ESR, Perkin Elmer, UK) with an EMCCD camera. Z stacks of 32–36 slices with 0.2 μm separation were acquired at one minute intervals for 70 min. Data analysis was performed using MetaMorph (MDS Analytical Technologies) and open source ImageJ software. Spindle elongation rates were determined as previously described [56]. The time between spindle elongation onset and the collapse of the spindle (i.e. disappearance of the midzone and decrease of the distance between the spindle poles) was considered as the time of spindle disassembly.

Analysis of fluorescence intensity distribution along the spindle

Line scan analysis parallel to the spindle was employed to quantify the distribution of 3GFP-tagged Cin8 variants and Spc42-tdTomato along the mitotic spindles, as previously described [71]. The fluorescence intensity profile was determined along a line tracing the spindle from mother to bud SPB. Corresponding bright field images were used to confirm mother-bud location (as shown in Fig. S1). For each mitotic spindle, the edges of the spindle were determined by the first and last intensity peaks of Cin8-3GFP fluorescence intensity or Spc42-tdTomato, representing the mother and bud SPBs, respectively. The background signal

was calculated by averaging the intensity outside the nucleus and subtracted that value from the fluorescence intensity measured at each point. Finally, intensity was interpolated and divided into 100 segments of equal length using Origin (OriginLab) software. Normalization of the Cin8-3GFP fluorescent signals was performed by dividing the intensity at each point by the total Cin8-3GFP fluorescence intensity at each spindle (Figs. 4, 5b; Fig. S6D) or by the maximal fluorescence intensity of Cin8-3GFP at each spindle (Fig. 3; Figs. S3B and S4). The average intensity was calculated for each length-point for 10–20 cells. To calculate the relative averaged intensity at the midzone, as in Figs. 3c and 4, the intensity of the normalized interpolated data was averaged between three points at the middle of the spindle length (i.e. points 49, 50 and 51 out of 100 interpolated points along the spindle length) for 10–20 cells. Statistical significances between the averages were determined by Student's *t* test.

Analysis of fluorescence intensity distribution perpendicular to the spindle

Line scan analysis perpendicular to the spindle was performed to quantify the detachment of Cin8 variants from the spindle during anaphase. First, the Cin8-3GFP fluorescence profile was measured along a line of 41 pixels (7.38 μm), drawn perpendicular to the spindle. The center of this line was set 2 pixels towards the midzone from a point of highest intensity, usually near the SPB (Fig. 6a). The intensity of the different regions along the line was categorized as follows: Twelve outer pixels on each side were assigned as background (Fig. 6a, burgundy rectangle). The intensity of 5 pixels in the center of the line was assigned as the intensity near the SPB or the spindle and was not considered in calculating Cin8 detachment (Fig. 6a, yellow rectangle). The intensities of pixels 12–18 and 23–29 were considered as the intensity resulting from Cin8-3GFP being localized in the nucleus due to its detachment from the spindle (Fig. 6a, green rectangle). Following subtraction of the background, the intensity along the line perpendicular to the spindle was normalized to the highest intensity value, usually observed near the SPB. Then, the intensity of Cin8-3GFP detached from the spindle (pixels 12–18 and 23–29) was averaged as a function of time for each cell. Finally, at each time point, the average nuclear Cin8-3GFP intensity in all cells expressing the same variant (9–12 cells) was calculated. Statistical significances between the averages were determined by Student's *t* test.

Yeast viability test

The viability of cells expressing the phospho-variants of Cin8 as a sole source of kinesin-5 function was performed as previously described [56, 81]. Yeast strains used for this

assay were deleted for chromosomal copies of *CIN8* and *KIP1* or *CIN8* and *ASE1*, and contained a recessive cycloheximide resistance gene and an initial plasmid encoding wt Cin8 and conferring cycloheximide sensitivity (plasmid pMA1208). As a result, this strain is sensitive to cycloheximide. After transformation with plasmids encoding Cin8 variants, the initial plasmid encoding wt Cin8 was shuffled out by growth on cycloheximide-containing medium. Prior to plating, cells were diluted to 0.2 O.D.$_{\lambda\,=\,600\,nm}$ (approximately 2.55×10^6 cells/mL). Then, additional serial dilution was performed for plating (1:1, 1:10, 1:10^2, 1:10^3, 1:10^4). Cells were grown on YPD medium containing 7.5 µg/mL cycloheximide for 3–4 days, at 26 and 37 °C.

Immunostaining

Immunostaining of the strains used in yeast viability assay was carried out as previously described [11, 95]. Following transformation with CEN plasmid expressing a particular phospho-variant, plasmid pMA1208 was shuffled out on YPD medium containing 7.5 µg/mL cycloheximide. A yeast culture at logarithmic growth phase (O.D.$_{\lambda\,=\,600\,nm}$ up to 0.2) was pelleted from liquid medium and fixed in 3.7% formaldehyde in phosphate-buffered solution (PBS; 40 mM K_2HPO_4, 10 mM KH_2PO_4, 0.15 M NaCl). Fixed cells were digested with zymolyase at 30 °C for 30 min (1.2 M sorbitol, 0.1 M KH_2PO_4, pH 7.5, 25 mM 2-mercaptoethanol, 50 µg/mL zymolyase 100T) and resuspended in PBS containing 0.1% BSA (PBS/BSA). Next, the cells were applied to polylysine-coated slides, washed with PBS/BSA, fixed in methanol and acetone at −20 °C and washed with PBS/BSA. MTs were labeled with monoclonal anti-tubulin rat YOL 1/34 IgG (Molecular Probes), as previously described and visualized with goat anti-rat IgG conjugated to Alexa 488 (ABD Serotec). DNA was visualized by washing the slides with PBS/BSA containing DAPI (1 µg/mL in PBS/BSA) for 5 min. The slides were mounted with p-phenylenediamine (1 mg/mL *p*-phenylenediamine in PBS, pH 9, 90% glycerol), and images were obtained using a Zeiss Axiovert 200 M-based microscope setup, as above. For each phospho-variant, the spindle and cell shape morphologies of 300 cells were categorized and counted. The percentages of the different spindle/cell shape categories were determined as a percentage from the total number of budded cells (150–200 budded cells in each experiment for each variant). Mitotic spindles were categorized by lengths and shape, and classified as monopolar, pre-anaphase (up to 2 µm in length), anaphase intermediate (2–5 µm in length) and anaphase long (5+ µm in length) spindles. Statistical analysis was based on three experiments.

References

1. Maddox P, Straight A, Coughlin P, Mitchison TJ, Salmon ED (2003) Direct observation of microtubule dynamics at kinetochores in *Xenopus* extract spindles: implications for spindle mechanics. J Cell Biol 162(3):377–382
2. Hoyt MA, He L, Loo KK, Saunders WS (1992) Two *Saccharomyces cerevisiae* kinesin-related gene products required for mitotic spindle assembly. J Cell Biol 118(1):109–120
3. Hagan I, Yanagida M (1992) Kinesin-related cut7 protein associates with mitotic and meiotic spindles in fission yeast. Nature 356(6364):74–76. doi:10.1038/356074a0
4. Heck MM, Pereira A, Pesavento P, Yannoni Y, Spradling AC, Goldstein LS (1993) The kinesin-like protein KLP61F is essential for mitosis in Drosophila. J Cell Biol 123(3):665–679
5. Blangy A, Lane HA, d'Herin P, Harper M, Kress M, Nigg EA (1995) Phosphorylation by p34cdc2 regulates spindle association of human Eg5, a kinesin-related motor essential for bipolar spindle formation in vivo. Cell 83(7):1159–1169
6. Goshima G, Vale RD (2005) Cell cycle-dependent dynamics and regulation of mitotic kinesins in Drosophila S2 cells. Mol Biol Cell 16(8):3896–3907
7. Scholey JE, Nithianantham S, Scholey JM, Al-Bassam J (2014) Structural basis for the assembly of the mitotic motor Kinesin-5 into bipolar tetramers. Elife 3:e02217. doi:10.7554/eLife.02217
8. Hildebrandt ER, Gheber L, Kingsbury T, Hoyt MA (2006) Homotetrameric form of Cin8p, a *Saccharomyces cerevisiae* kinesin-5 motor, is essential for its in vivo function. J Biol Chem 281(36):26004–26013
9. Gordon DM, Roof DM (1999) The kinesin-related protein Kip1p of *Saccharomyces cerevisiae* is bipolar. J Biol Chem 274(40):28779–28786
10. Kashina AS, Baskin RJ, Cole DG, Wedaman KP, Saxton WM, Scholey JM (1996) A bipolar kinesin. Nature 379(6562):270–272
11. Gheber L, Kuo SC, Hoyt MA (1999) Motile properties of the kinesin-related Cin8p spindle motor extracted from *Saccharomyces cerevisiae* cells. J Biol Chem 274(14):9564–9572
12. Kapitein LC, Peterman EJ, Kwok BH, Kim JH, Kapoor TM, Schmidt CF (2005) The bipolar mitotic kinesin Eg5 moves on both microtubules that it crosslinks. Nature 435(7038):114–118
13. Roof DM, Meluh PB, Rose MD (1992) Kinesin-related proteins required for assembly of the mitotic spindle. J Cell Biol 118:95–108
14. Saunders WS, Hoyt MA (1992) Kinesin-related proteins required for structural integrity of the mitotic spindle. Cell 70(3):451–458
15. Saunders WS, Koshland D, Eshel D, Gibbons IR, Hoyt MA (1995) *Saccharomyces cerevisiae* kinesin- and dynein-related proteins required for anaphase chromosome segregation. J Cell Biol 128(4):617–624
16. Gerson-Gurwitz A, Movshovich N, Avunie R, Fridman V, Moyal K, Katz B, Hoyt MA, Gheber L (2009) Mid-anaphase arrest in S. cerevisiae cells eliminated for the function of Cin8 and dynein. Cell Mol Life Sci 66(2):301–313

17. Movshovich N, Fridman V, Gerson-Gurwitz A, Shumacher I, Gertsberg I, Fich A, Hoyt MA, Katz B, Gheber L (2008) Slk19-dependent mid-anaphase pause in kinesin-5-mutated cells. J Cell Sci 121(15):2529–2539

18. Straight AF, Sedat JW, Murray AW (1998) Time-lapse microscopy reveals unique roles for kinesins during anaphase in budding yeast. J Cell Biol 143(3):687–694

19. Fridman V, Gerson-Gurwitz A, Movshovich N, Kupiec M, Gheber L (2009) Midzone organization restricts interpolar microtubule plus-end dynamics during spindle elongation. EMBO Rep 10(4):387–393

20. Gardner MK, Bouck DC, Paliulis LV, Meehl JB, O'Toole ET, Haase J, Soubry A, Joglekar AP, Winey M, Salmon ED, Bloom K, Odde DJ (2008) Chromosome congression by Kinesin-5 motor-mediated disassembly of longer kinetochore microtubules. Cell 135(5):894–906

21. Wargacki MM, Tay JC, Muller EG, Asbury CL, Davis TN (2010) Kip3, the yeast kinesin-8, is required for clustering of kinetochores at metaphase. Cell Cycle 9(13):2581–2588

22. Tytell JD, Sorger PK (2006) Analysis of kinesin motor function at budding yeast kinetochores. JCB 172(6):861–874

23. Gibbs KL, Greensmith L, Schiavo G (2015) Regulation of axonal transport by protein kinases. Trends Biochem Sci 40(10):597–610. doi:10.1016/j.tibs.2015.08.003

24. Morfini G, Schmidt N, Weissmann C, Pigino G, Kins S (2016) Conventional kinesin: biochemical heterogeneity and functional implications in health and disease. Brain Res Bull. doi:10.1016/j.brainresbull.2016.06.009

25. Ritter A, Kreis NN, Louwen F, Wordeman L, Yuan J (2015) Molecular insight into the regulation and function of MCAK. Crit Rev Biochem Mol Biol 51(4):228–245. doi:10.1080/10409238.2016.1178705

26. Waitzman JS, Rice SE (2014) Mechanism and regulation of kinesin-5, an essential motor for the mitotic spindle. Biol Cell 106(1):1–12. doi:10.1111/boc.201300054

27. Wojcik EJ, Buckley RS, Richard J, Liu L, Huckaba TM, Kim S (2013) Kinesin-5: cross-bridging mechanism to targeted clinical therapy. Gene 531(2):133–149. doi:10.1016/j.gene.2013.08.004

28. Manser C, Guillot F, Vagnoni A, Davies J, Lau KF, McLoughlin DM, De Vos KJ, Miller CC (2012) Lemur tyrosine kinase-2 signalling regulates kinesin-1 light chain-2 phosphorylation and binding of Smad2 cargo. Oncogene 31(22):2773–2782. doi:10.1038/onc.2011.437

29. Craige B, Witman GB (2014) Flipping a phosphate switch on kinesin-II to turn IFT around. Dev Cell 30(5):492–493. doi:10.1016/j.devcel.2014.08.019

30. Fesquet D, De Bettignies G, Bellis M, Espeut J, Devault A (2015) Binding of Kif23-iso1/CHO1 to 14-3-3 is regulated by sequential phosphorylations at two LATS kinase consensus sites. PLoS One 10(2):e0117857. doi:10.1371/journal.pone.0117857

31. Ogawa T, Hirokawa N (2015) Microtubule destabilizer KIF2A undergoes distinct site-specific phosphorylation cascades that differentially affect neuronal morphogenesis. Cell Rep 12(11):1774–1788. doi:10.1016/j.celrep.2015.08.018

32. Drechsler H, Tan AN, Liakopoulos D (2015) Yeast GSK-3 kinase regulates astral microtubule function through phosphorylation of the microtubule-stabilizing kinesin Kip2. J Cell Sci 128(21):3910–3921. doi:10.1242/jcs.166686

33. Zong H, Carnes SK, Moe C, Walczak CE, Ems-McClung SC (2016) The far C-terminus of MCAK regulates its conformation and spindle pole focusing. Mol Biol Cell 27(9):1451–1464. doi:10.1091/mbc.E15-10-0699

34. Cantuti Castelvetri L, Givogri MI, Hebert A, Smith B, Song Y, Kaminska A, Lopez-Rosas A, Morfini G, Pigino G, Sands M, Brady ST, Bongarzone ER (2013) The sphingolipid psychosine inhibits fast axonal transport in Krabbe disease by activation of GSK3beta and deregulation of molecular motors. J Neurosci 33(24):10048–10056. doi:10.1523/JNEUROSCI.0217-13.2013

35. Morfini G, Szebenyi G, Elluru R, Ratner N, Brady ST (2002) Glycogen synthase kinase 3 phosphorylates kinesin light chains and negatively regulates kinesin-based motility. EMBO J 21(3):281–293. doi:10.1093/emboj/21.3.281

36. Pigino G, Morfini G, Atagi Y, Deshpande A, Yu C, Jungbauer L, LaDu M, Busciglio J, Brady S (2009) Disruption of fast axonal transport is a pathogenic mechanism for intraneuronal amyloid beta. Proc Natl Acad Sci USA 106(14):5907–5912. doi:10.1073/pnas.0901229106

37. Morfini GA, Bosco DA, Brown H, Gatto R, Kaminska A, Song Y, Molla L, Baker L, Marangoni MN, Berth S, Tavassoli E, Bagnato C, Tiwari A, Hayward LJ, Pigino GF, Watterson DM, Huang CF, Banker G, Brown RH Jr, Brady ST (2013) Inhibition of fast axonal transport by pathogenic SOD1 involves activation of p38 MAP kinase. PLoS One 8(6):e65235. doi:10.1371/journal.pone.0065235

38. Morfini G, Pigino G, Szebenyi G, You Y, Pollema S, Brady ST (2006) JNK mediates pathogenic effects of polyglutamine-expanded androgen receptor on fast axonal transport. Nat Neurosci 9(7):907–916. doi:10.1038/nn1717

39. Morfini GA, You YM, Pollema SL, Kaminska A, Liu K, Yoshioka K, Bjorkblom B, Coffey ET, Bagnato C, Han D, Huang CF, Banker G, Pigino G, Brady ST (2009) Pathogenic huntingtin inhibits fast axonal transport by activating JNK3 and phosphorylating kinesin. Nat Neurosci 12(7):864–871. doi:10.1038/nn.2346

40. Courtheoux T, Gay G, Reyes C, Goldstone S, Gachet Y, Tournier S (2007) Dynein participates in chromosome segregation in fission yeast. Biol Cell 99(11):627–637

41. Padzik A, Deshpande P, Hollos P, Franker M, Rannikko EH, Cai D, Prus P, Magard M, Westerlund N, Verhey KJ, James P, Hoogenraad CC, Coffey ET (2016) KIF5C S176 phosphorylation regulates microtubule binding and transport efficiency in mammalian neurons. Front Cell Neurosci 10:57. doi:10.3389/fncel.2016.00057

42. Han X, Adames K, Sykes EM, Srayko M (2015) The KLP-7 residue S546 is a putative aurora kinase site required for microtubule regulation at the centrosome in C. elegans. PLoS One 10(7):e0132593. doi:10.1371/journal.pone.0132593

43. Andrews PD, Ovechkina Y, Morrice N, Wagenbach M, Duncan K, Wordeman L, Swedlow JR (2004) Aurora B regulates MCAK at the mitotic centromere. Dev Cell 6(2):253–268

44. Lan W, Zhang X, Kline-Smith SL, Rosasco SE, Barrett-Wilt GA, Shabanowitz J, Hunt DF, Walczak CE, Stukenberg PT (2004) Aurora B phosphorylates centromeric MCAK and regulates its localization and microtubule depolymerization activity. Curr Biol 14(4):273–286

45. Ohi R, Sapra T, Howard J, Mitchison TJ (2004) Differentiation of cytoplasmic and meiotic spindle assembly MCAK functions by Aurora B-dependent phosphorylation. Mol Biol Cell 15(6):2895–2906. doi:10.1091/mbc.E04-02-0082

46. Zhang X, Ems-McClung SC, Walczak CE (2008) Aurora A phosphorylates MCAK to control ran-dependent spindle bipolarity. Mol Biol Cell 19(7):2752–2765. doi:10.1091/mbc.E08-02-0198

47. Mennella V, Tan DY, Buster DW, Asenjo AB, Rath U, Ma A, Sosa HJ, Sharp DJ (2009) Motor domain phosphorylation and regulation of the Drosophila kinesin 13, KLP10A. J Cell Biol 186(4):481–490

48. Ritter A, Sanhaji M, Friemel A, Roth S, Rolle U, Louwen F, Yuan J (2015) Functional analysis of phosphorylation of the mitotic centromere-associated kinesin by Aurora B kinase in human tumor cells. Cell Cycle 14(23):3755–3767. doi:10.1080/15384101.2015.1068481

49. Sanhaji M, Friel CT, Kreis NN, Kramer A, Martin C, Howard J, Strebhardt K, Yuan J (2010) Functional and spatial regulation of mitotic centromere-associated kinesin by cyclin-dependent kinase 1. Mol Cell Biol 30(11):2594–2607

50. Giet R, Uzbekov R, Cubizolles F, Le Guellec K, Prigent C (1999) The *Xenopus laevis* aurora-related protein kinase pEg2 associates with and phosphorylates the kinesin-related protein XlEg5. J Biol Chem 274(21):15005–15013

51. Sharp DJ, McDonald KL, Brown HM, Matthies HJ, Walczak C, Vale RD, Mitchison TJ, Scholey JM (1999) The bipolar kinesin, KLP61F, cross-links microtubules within interpolar microtubule bundles of Drosophila embryonic mitotic spindles. J Cell Biol 144(1):125–138

52. Sawin KE, Mitchison TJ (1995) Mutations in the kinesin-like protein Eg5 disrupting localization to the mitotic spindle. Proc Natl Acad Sci USA 92(10):4289–4293

53. Cahu J, Olichon A, Hentrich C, Schek H, Drinjakovic J, Zhang C, Doherty-Kirby A, Lajoie G, Surrey T (2008) Phosphorylation by Cdk1 increases the binding of Eg5 to microtubules in vitro and in Xenopus egg extract spindles. PLoS One 3(12):e3936

54. Bishop JD, Han Z, Schumacher JM (2005) The Caenorhabditis elegans Aurora B kinase AIR-2 phosphorylates and is required for the localization of a BimC kinesin to meiotic and mitotic spindles. Mol Biol Cell 16(2):742–756

55. Drummond DR, Hagan IM (1998) Mutations in the bimC box of Cut7 indicate divergence of regulation within the bimC family of kinesin related proteins. J Cell Sci 111(Pt 7):853–865

56. Avunie-Masala R, Movshovich N, Nissenkorn Y, Gerson-Gurwitz A, Fridman V, Koivomagi M, Loog M, Hoyt MA, Zaritsky A, Gheber L (2011) Phospho-regulation of kinesin-5 during anaphase spindle elongation. J Cell Sci 124(Pt 6):873–878

57. Olsen JV, Vermeulen M, Santamaria A, Kumar C, Miller ML, Jensen LJ, Gnad F, Cox J, Jensen TS, Nigg EA, Brunak S, Mann M (2010) Quantitative phosphoproteomics reveals widespread full phosphorylation site occupancy during mitosis. Sci Signal 3(104):ra3. doi:10.1126/scisignal.2000475

58. Smith E, Hegarat N, Vesely C, Roseboom I, Larch C, Streicher H, Straatman K, Flynn H, Skehel M, Hirota T, Kuriyama R, Hochegger H (2011) Differential control of Eg5-dependent centrosome separation by Plk1 and Cdk1. EMBO J 30(11):2233–2245. doi:10.1038/emboj.2011.120

59. Kahn OI, Sharma V, Gonzalez-Billault C, Baas PW (2015) Effects of kinesin-5 inhibition on dendritic architecture and microtubule organization. Mol Biol Cell 26(1):66–77. doi:10.1091/mbc.E14-08-1313

60. Garcia K, Stumpff J, Duncan T, Su TT (2009) Tyrosines in the kinesin-5 head domain are necessary for phosphorylation by Wee1 and for mitotic spindle integrity. Curr Biol 19(19):1670–1676

61. Chee MK, Haase SB (2010) B-cyclin/CDKs regulate mitotic spindle assembly by phosphorylating kinesins-5 in budding yeast. PLoS Genet 6:e1000935

62. Shapira O, Gheber L (2016) Motile properties of the bi-directional kinesin-5 Cin8 are affected by phosphorylation in its motor domain. Sci Rep 6(25597):25597

63. Schuyler SC, Liu JY, Pellman D (2003) The molecular function of Ase1p: evidence for a MAP-dependent midzone-specific spindle matrix. Microtubule-associated proteins. J Cell Biol 160(4):517–528

64. Khmelinskii A, Roostalu J, Roque H, Antony C, Schiebel E (2009) Phosphorylation-dependent protein interactions at the spindle midzone mediate cell cycle regulation of spindle elongation. Dev Cell 17(2):244–256

65. Kull FJ, Sablin EP, Lau R, Fletterick RJ, Vale RD (1996) Crystal structure of the kinesin motor domain reveals a structural similarity to myosin. Nature 380(6574):550–555

66. Sablin EP, Kull FJ, Cooke R, Vale RD, Fletterick RJ (1996) Crystal structure of the motor domain of the kinesin-related motor ncd. Nature 380(6574):555–559

67. Roostalu J, Hentrich C, Bieling P, Telley IA, Schiebel E, Surrey T (2011) Directional switching of the Kinesin cin8 through motor coupling. Science 332(6025):94–99

68. Gerson-Gurwitz A, Thiede C, Movshovich N, Fridman V, Podolskaya M, Danieli T, Lakamper S, Klopfenstein DR, Schmidt CF, Gheber L (2011) Directionality of individual kinesin-5 Cin8 motors is modulated by loop 8, ionic strength and microtubule geometry. EMBO J 30(24):4942–4954

69. Shapira O, Goldstein A, Al-Bassam J, Gheber L (2017) A potential physiological role for bi-directional motility and motor clustering of mitotic kinesin-5 Cin8 in yeast mitosis. J Cell Sci 130(4):725–734

70. Konig C, Maekawa H, Schiebel E (2010) Mutual regulation of cyclin-dependent kinase and the mitotic exit network. J Cell Biol 188(3):351–368

71. Fridman V, Gerson-Gurwitz A, Shapira O, Movshovich N, Lakamper S, Schmidt CF, Gheber L (2013) Kinesin-5 Kip1 is a bi-directional motor that stabilizes microtubules and tracks their plus-ends in vivo. J Cell Sci 126(Pt 18):4147–4159. doi:10.1242/jcs.125153

72. Hildebrandt ER, Hoyt MA (2001) Cell cycle-dependent degradation of the *Saccharomyces cerevisiae* spindle motor Cin8p requires APC(Cdh1) and a bipartite destruction sequence. Mol Biol Cell 12(11):3402–3416

73. Diogo V, Teixeira J, Silva PM, Bousbaa H (2016) Spindle assembly checkpoint as a potential target in colorectal cancer: current status and future perspectives. Clin Colorectal Cancer 23(16):30080–30089

74. Musacchio A (2015) The molecular biology of spindle assembly checkpoint signaling dynamics. Curr Biol 25(20):R1002–R1018

75. Topham CH, Taylor SS (2013) Mitosis and apoptosis: how is the balance set? Curr Opin Cell Biol 25(6):780–785. doi:10.1016/j.ceb.2013.07.003

76. Bardin AJ, Amon A (2001) Men and sin: what's the difference? Nat Rev Mol Cell Biol 2(11):815–826. doi:10.1038/35099020

77. Hotz M, Leisner C, Chen D, Manatschal C, Wegleiter T, Ouellet J, Lindstrom D, Gottschling DE, Vogel J, Barral Y (2012) Spindle pole bodies exploit the mitotic exit network in metaphase to drive their age-dependent segregation. Cell 148(5):958–972

78. Segal M (2011) Mitotic exit control: a space and time odyssey. Curr Biol 21(20):R857–R859. doi:10.1016/j.cub.2011.09.023

79. Gigant B, Wang W, Dreier B, Jiang Q, Pecqueur L, Pluckthun A, Wang C, Knossow M (2013) Structure of a kinesin-tubulin complex and implications for kinesin motility. Nat Struct Mol Biol 20(8):1001–1007

80. Zhang X, Lan W, Ems-McClung SC, Stukenberg PT, Walczak CE (2007) Aurora B phosphorylates multiple sites on mitotic centromere-associated kinesin to spatially and temporally regulate its function. Mol Biol Cell 18(9):3264–3276. doi:10.1091/mbc.E07-01-0086

81. Duselder A, Fridman V, Thiede C, Wiesbaum A, Goldstein A, Klopfenstein DR, Zaitseva O, Janson ME, Gheber L, Schmidt CF (2015) Deletion of the tail domain of the kinesin-5 Cin8 affects its directionality. J Biol Chem 19:620799

82. Thiede C, Fridman V, Gerson-Gurwitz A, Gheber L, Schmidt CF (2012) Regulation of bi-directional movement of single kinesin-5 Cin8 molecules. Bioarchitecture 2(2):70–74

83. Queralt E, Lehane C, Novak B, Uhlmann F (2006) Downregulation of PP2A(Cdc55) phosphatase by separase initiates mitotic exit in budding yeast. Cell 125(4):719–732

84. Chiroli E, Rancati G, Catusi I, Lucchini G, Piatti S (2009) Cdc14 inhibition by the spindle assembly checkpoint prevents unscheduled centrosome separation in budding yeast. Mol Biol Cell 20(10):2626–2637

85. Roccuzzo M, Visintin C, Tili F, Visintin R (2015) FEAR-mediated activation of Cdc14 is the limiting step for spindle elongation and anaphase progression. Nat Cell Biol 17(3):251–261. doi:10.1038/ncb3105

86. Ross KE, Cohen-Fix O (2004) A role for the FEAR pathway in nuclear positioning during anaphase. Dev Cell 6(5):729–735

87. D'Amours D, Amon A (2004) At the interface between signaling and executing anaphase—Cdc14 and the FEAR network. Genes Dev 18(21):2581–2595

88. Yellman CM, Roeder GS (2015) Cdc14 early anaphase release, FEAR, is limited to the nucleus and dispensable for efficient mitotic exit. PLoS One 10(6):e0128604

89. Stegmeier F, Visintin R, Amon A (2002) Separase, polo kinase, the kinetochore protein Slk19, and Spo12 function in a network that controls Cdc14 localization during early anaphase. Cell 108(2):207–220

90. Pellman D, Bagget M, Tu YH, Fink GR, Tu H (1995) Two microtubule-associated proteins required for anaphase spindle movement in *Saccharomyces cerevisiae*. J Cell Biol 130(6):1373–1385

91. Fu C, Ward JJ, Loiodice I, Velve-Casquillas G, Nedelec FJ, Tran PT (2009) Phospho-regulated interaction between kinesin-6 Klp9p and microtubule bundler Ase1p promotes spindle elongation. Dev Cell 17(2):257–267

92. Rozelle DK, Hansen SD, Kaplan KB (2011) Chromosome passenger complexes control anaphase duration and spindle elongation via a kinesin-5 brake. J Cell Biol 193(2):285–294

93. Saunders AM, Powers J, Strome S, Saxton WM (2007) Kinesin-5 acts as a brake in anaphase spindle elongation. Curr Biol 17(12):R453–R454

94. Shimamoto Y, Forth S, Kapoor TM (2015) Measuring pushing and braking forces generated by ensembles of kinesin-5 crosslinking two microtubules. Dev Cell 34(6):669–681

95. Cottingham FR, Gheber L, Miller DL, Hoyt MA (1999) Novel roles for *Saccharomyces cerevisiae* mitotic spindle motors. J Cell Biol 147(2):335–350